Thermodynamics of magnetic chains with $S \leq 5/2$

T. de Neef*
Department of Physics, Eindhoven University of Technology, Eindhoven, The Netherlands
(Received 5 August 1974; revised manuscript received 7 July 1975)

The specific heat (C) and entropy (η) in zero field are calculated for infinite chains of spins, coupled by a nearest-neighbor Heisenberg exchange. The data presented include all spin values $S \leq 5/2$ and cover ferromagnetic and antiferromagnetic exchange. Several techniques are used to obtain reliable estimates for the infinite chains, and much attention is given to the theory underlying these techniques. For high temperatures the series expansion of C is used for the estimates. Coefficients in the series are obtained from the energy spectra of different finite chains. This method is fully described, and attention is given to the estimation of further coefficients. For intermediate temperatures, around the region where C displays the characteristic broad maximum, the series expansions fail and here the estimates of the infinite chain are obtained from a suitable extrapolation of the data for finite chains. This method is shown to be correct for sufficiently high temperatures. It is applicable to a wide temperature range. For temperatures near $T = 0$, C is described by a polynomial based on the spin-wave theory. The coefficients in this polynomial are equated such that a smooth fit in with the intermediate temperature specific heat is obtained and that at the same time the over-all entropy gain is correct. The results are, as far as possible, tabulated.

I. INTRODUCTION

An ensemble of an infinite number of spins with interactions is most easily studied theoretically in the two limiting cases of a one-dimensional (1-d) arrangement and of an infinite-dimensional lattice. The second case, known as the equivalent-neighbor model,[1] has little practical application, but in experimental magnetism several compounds are known to approach a 1-d model.[2] Theoretical attention to 1-d systems started, long before any experimental need for such models existed, with the solution of the partition function of the Ising model with $S = \frac{1}{2}$.[3] Since then, several other models have been solved,[4] but in spite of much effort, few general solutions have been arrived at. The best-known examples are those of the XY Hamiltonian for $S = \frac{1}{2}$ in zero field[5] and the classical limit of infinite spins interacting isotropically in D dimensions of the spin vector space.[6-8] The generalized Ising Hamiltonian with additional single-ion interactions (magnetic field or zero-field splitting) can be solved in principle for any spin quantum number using the transfer-matrix technique.[9] For several other models less-detailed information exists,[4] such as the ground-state energy or the susceptibility for $T = 0$.

The experimental study of crystals with a nearly-1-d behavior started on substances with Cu^{2+} as the magnetic ion.[10,11] Since Cu^{2+} ($S = \frac{1}{2}$) generally displays a Heisenberg or anisotropic exchange, approximate techniques were had recourse to in order to enable a comparison between theory and experiments to be made.

Series expansion for the isotropic[12] and the anisotropic[13,14] Hamiltonians offered the possibility of such comparison for the high-temperature side. The estimates of Bonner and Fisher,[15] based on extrapolation of the data for finite rings of spins, covered also temperatures well below the characteristic broad maxima in the specific heat (C) and susceptibility (χ).

The study of crystals with other magnetic ions has resulted in the discovery of fairly good approximations of 1-d Heisenberg models, such as TMMC[16,17] (tetramethyl ammonium manganese chloride) and CMC[18,19] (cesium manganese chloride). Such systems ($S = \frac{5}{2}$) are confronted with a further lack of theoretical predictions. The series-expansion work of Rushbrooke and Wood[20] gives information concerning the high-temperature behavior, but for lower temperatures the information is limited, when $S > \frac{1}{2}$.

For $S = 1$, Weng[21] studied C and χ for the isotropic case. Stimulated by the experiments on salts with Ni^{2+} as the magnetic ion, we have recently presented estimates of C for an $S = 1$ Hamiltonian with isotropic exchange and a zero-field splitting term ΔS_z^2.[22] Green's-function analysis by Rhodes and Scales[23] offers some data for $S = \frac{5}{2}$.

Our main interest lies in the behavior of chains with nearest-neighbor Heisenberg interactions and spin $S = \frac{5}{2}$ (Mn^{2+}, Fe^{3+}).[24] Since Bonner and Fisher's technique was shown to yield fair results for $S = 1$,[21,22,25] it was examined to see if this method was worthwhile for $S = \frac{5}{2}$ too. This actually turned out to be the case, but in order to get a general feeling about the uncertaintites in the estimate of C, we employed this technique for all smaller spin quantum numbers as well.

In order to estimate C for the infinite chain, we did not restrict ourselves to the technique of extrapolation from finite chains and rings. For the high-temperature side, the series expansion in β $(=1/kT)$ was derived from the calculated properties of finite chains. The region near $T=0$ is hardest to examine. There we used a polynomial in T based on spin-wave theory,[26] the coefficients of which are chosen so as to assure the correct entropy gain and a smooth transition to estimates for higher temperatures. We quote a possible error of about 5% below T_m (the temperature for which C is maximum), 0.5% in its neighborhood, and no error for $T > \frac{3}{2} T_m$, for $S = \frac{5}{2}$.

For $S < \frac{5}{2}$ the error in the low-temperature region gradually increases, especially for the antiferromagnetic chain. For $S = \frac{1}{2}$, the (antiferromagnetic) polynomial fitting must even be considered unreliable.

In order to defend the estimates, much attention is given to the application of the different methods, and this finds its clear display in the grouping of the chapters. Instead of a division starting from spin quantum number or sign of the exchange, we preferred a presentation based on temperature region. After a general theoretical introduction, attention is turned to the high-temperature region $(T \gg T_m)$ and the series expansions of C are discussed. The technique of extrapolation of the results for finite chains is typical of intermediate temperatures $(T \simeq T_m)$, which are reviewed in Sec. IV. The low-temperature side $(T < T_m)$ will be discussed in Sec. V and in Sec. VI we present the over-all estimates and compare them with others.

II. GENERAL REMARKS

The common features of all systems studied here are the 1-d arrangement of spins and the absence of any anisotropy in the exchange interaction. The interaction is between nearest neighbors only and a magnetic field is not present. For chains the Hamiltonian can be written as

$$\mathcal{H} = -2J \sum_{i=1}^{N-1} \vec{S}_i \cdot \vec{S}_{i+1} \,. \tag{1}$$

When dealing with rings the additional interaction between $\vec{S}_1$ and $\vec{S}_N$ is included.

The exchange J may be of ferromagnetic sign $(J>0)$ or antiferromagnetic $(J<0)$ and the spin S ranges from $S=\frac{1}{2}$ to $S=\frac{5}{2}$. In estimating the thermodynamic behavior of the 1-d system when $N \to \infty$, use will be made of the data for finite clusters of spins. To calculate the thermal behavior of these systems, a detailed knowledge of the eigenvalue spectrum for given N and S is a prerequisite and we shall first consider the limitations imposed on this calculation. For N spins S there are $(2S+1)^N$ eigenvalues, and they can be found by diagonalization of the matrix representation of $\mathcal{H}$ on any set of basis functions. The use of good quantum numbers may facilitate such diagonalization since it will result in factorization of the matrix. Owing to the completely isotropic character of the interactions, good quantum numbers are $\vec{T}^2$ and T_z $(\vec{T} = \sum_i \vec{S}_i)$. These are independent of the precise topological way the spins are coupled. Further factorization may be accomplished by using the symmetry of the cluster. For a chain, an inversion center exists, and parity would be a good quantum number: eigenfunctions of $\mathcal{H}$ transform according to the irreducible representations (IR) of the group D_2. The translational invariance of a ring makes the wave vector $\vec{k}$ as well as the IR's of the group D_N good quantum numbers. The higher symmetry of a ring allows of a solution of the eigenvalue spectrum for a system with more spins than is possible for a chain. However, it appears that in practical computations not all good quantum numbers should be used to obtain minimum computer time. The good quantum numbers can be introduced in two ways, which we shall briefly describe here.

The first is to construct basis functions that are eigenfunctions of T_z, project them on one of the IR of the group associated with $\mathcal{H}$, and finally apply a projection after total spin T. The first projection can be obtained using ordinary group-theoretical methods (since the functions are already eigenfunctions of T_z, only positional permutations of the spins are of importance, and use of double groups can be avoided). The projection of a function on the subspace of a certain total spin T may be accomplished with the aid of the projector P_T,

$$P_T = \prod_{S \neq T} [\vec{S}^2 - S(S+1)] \,. \tag{2}$$

Since any eigenfunction of $T_z \propto M_T$ can contain only functions that belong to $T > M_T$, the product may even be limited to $S > T$.

The second possibility consists in constructing eigenfunctions of $\vec{T}^2$ and T_z in the first stage by applying Clebsch-Gordan coefficients[27] and in using in the second stage the group symmetry. In both cases further use can be made of the commutation of $\mathcal{H}$ and $\vec{T}^2$, since this guarantees that any eigenvalue for the solution in the subspace with $T_z \propto M_T$ will reappear in the problem with $M_T' < M_T$ [all eigenvalues belonging to a certain total spin T are $(2T+1)$-fold degenerate]. Of these two possible approaches to the solution, the first is preferable for the matter of program generality,

since it results in a program that can handle any Hamiltonian showing axial symmetry. The first projection is then applied according to the symmetry group of $\mathcal{H}$ and the second may be used if $[\mathcal{H}, \vec{T}^2] = 0$, as in the present study. This has been the set up of our main programs. It turned out, however, that the application of P_T is so elaborate that it consumes all computer time saved in the solution of a smaller eigenvalue equation. For large N, therefore, the second scheme had to be used and there the symmetry of $\mathcal{H}$ had to be omitted for the same reasons.

The maximum allowable number of spins in a cluster is determined by the resulting order of the largest eigenvalue problem, together with computer limitations. A summary of these numbers is given in Table I for rings and chains.

Once the complete set of eigenvalues is known, the partition function may be calculated from

$$Z_N = \sum_i e^{-\beta E_i} ,$$

the summation being over all $(2S+1)^N$ energy levels.

TABLE I. Summary of the order of the largest eigenvalue problem arising in the solution of the energy spectrum of finite rings and chains with various spin. The columns headed A give these numbers when use is made of the topological symmetry of the clusters (group D_2 for chains, D_N for rings of N spins) but not of the commutivity of $\mathcal{H}$ and $\vec{T}^2$. Column B lists the order of the largest eigenvalue equation when the symmetry of the clusters is not taken into account, but $[\mathcal{H}, \vec{T}^2] = 0$ and $[\mathcal{H}, T_z] = 0$ is used. In this case no difference exists between rings and chains. Underlined numbers in the second column indicate that it has been possible to calculate the eigenvalues for rings as well as for chains. In the other cases only rings could be solved.

S	N	A (ring)	A (chain)	B
$\frac{1}{2}$	9	10	66	48
	10	25	126	90
	11	44	236	165
	12	78		297
	13	138		572
1	6	24	74	40
	7	56	200	105
	8	140		280
$\frac{3}{2}$	5	31	81	36
	6	96		120
2	4	19	45	17
	5	76	197	70
$\frac{5}{2}$	4	35	76	24
	5	156		120

The thermodynamic functions are then found from the Gibbs free energy $[G_N = -\ln(Z_N)/\beta]$ and its derivatives. Naturally, all these functions give detailed information only for the finite systems they are derived from. The main task in finding the behavior of an infinite chain is either to eliminate the boundary effects in case of a chain calculation or to extend the finite $\vec{k}$ spectrum to its continuous limit when dealing with rings. This happens to be possible in the two limits $\beta \to 0$ and $T \to 0$, at least in principle. The high-temperature region ($\beta J \ll S^2$) is most easily analyzed by using a perturbation series. Since in this limit all functions for magnetic systems attain constant values, they may be expanded into a power series in β. The coefficients of the ensuing expansions [high-temperature expansions (HTE)] for the infinite chain can be expressed in traces of the Hamiltonian for finite clusters, which makes possible an indirect extrapolation to the case $N \to \infty$. Section III will be devoted to this matter.

For temperatures near $T = 0$ a convenient approach is the assumption of spin waves and calculation of their dispersion relation. It is generally assumed that this technique yields fair results for 3-d lattices but for a 1-d arrangement of spins the predictions turn out to be only of qualitative correctness. Studies in this low-temperature limit will be the subject of Sec. V.

It appears that the HTE, although covering a considerable part of the temperature scale, is not powerful enough to reach the spin-wave region and one is left with the intermediate temperatures ($\beta J \simeq S^2$). Estimates of the limiting function in this region may be obtained by using Padé approximants of the HTE. This will be discussed in Sec. IV, where we shall also show that an even more powerful method is possible if the data for finite chains are used directly.

III. HIGH-TEMPERATURE REGION

In the extreme limit of $\beta \to 0$, all energy levels are equally populated and the partition function Z is just the total number of levels. For increasing β, $Z(\beta)$ may then be expressed in a power series and all thermodynamic functions can be found by suitable differentiation of this series. We shall turn our attention mainly to the specific heat per site (C) and for that quantity the first term in the series is in β^2,

$$C \sim \sum_{i=2}^{M} a_i K^i , \tag{3}$$

with $K = \beta J$. The series is infinite but in actual calculations M will be finite. The number of computable terms depends on the technique of calcu-

lating the coefficients. Each coefficient a_i is related to the trace of the ith power of $\mathcal{H}$, which can be solved by diagrammatic techniques. A straightforward calculation after the general rules of Rushbrooke and Wood[20] limits us to a maximum of $M=11$ for general spin. However, once the Hamiltonian is solved for a number of finite chains, the coefficients may be calculated directly from the eigenvalues and the maximum M is then related with the maximum size N of a chain through $M=2N-1$. Owing to the properties of one of the contributing graphs, one further term may be found approximatively. For $S=\frac{1}{2}$, this sets the maximum to $M=22$.

For calculating the coefficients two approaches are available. The simplest (the cumulant method) was originally proposed by Domb[28] and, for $S=\frac{1}{2}$ chains, applied by Baker *et al.*[29] It consists of an expansion of the Gibbs free energy for the infinite lattice in terms of the corresponding quantity for a number of finite lattices. The attractiveness of this approach is that only the occurrence of connected linear graphs is of interest.[30]

The second approach is directly related with the expansion of C in traces of $\mathcal{H}$, $\mathcal{H}^2$, etc., as introduced by Opechowski[31] (moment method). Here too the basic units (the trace of certain graphs) are calculated by a suitable combination of the traces of $\mathcal{H}$ for a number of finite lattices. In this case not only the occurrence of connected graphs is of importance but also that of disconnected ones. Although this involves a far more complex calculation scheme, it is worth applying since it can serve as a check on any systematic or rounding errors in the calculation after Domb. Furthermore, this method allows us to calculate one more coefficient in the series. Since for both schemes the procedure is one of recursive calculation, propagation of rounding errors may be severe. We shall first outline the principles in more detail and turn to the error propagation afterwards. In the following subsections the definitions and formal solution for both schemes are described, starting with the moment method.

A. Moment method: Definitions and notation

The normalized trace of the nth power of $\mathcal{H}_N$ will be denoted by

$$\mathrm{tr}(\mathcal{H}_N^n)=(2S+1)^{-N}\sum_i E_i^n \ . \tag{4}$$

Each trace can be divided in contributions from different clusters in the chain. This is conveniently done by the introduction of graphs. Each term $J(\vec{S}_i\cdot\vec{S}_{i+1})$ is therefore represented by a bar connecting sites i and $i+1$. If all n sites in a graph in $\mathrm{tr}(\mathcal{H}_N^n)$ are interconnected, we shall call the graph simple and denote its trace by $d(n)$. In order to distinguish between different graphs of the same order, they will be labeled according to their length: $d_l(n)$ for a graph with all sites interconnected and between points i and $i+l$ on the lattice.[32] When the sites in a graph are not all interconnected, the graph will be called composite, and its trace denoted by $D_{\vec{\Gamma}}(n)$. The vector subscript indicates the lengths of the set of composing simple graphs. The decomposition into simple graphs enables a relation between $D_{\vec{\Gamma}}(n)$ and $d_l(k)$ to be expressed:

$$\begin{aligned} D_{\vec{\Gamma}}(n) &= D_{l_1,l_2,l_3,\ldots,l_m}(n) \\ &= n!\sum_{\vec{r}}\gamma_n(r_1,r_2,\ldots,r_m)\prod_{i,j}\frac{d_{l_i}(r_j)}{r_j!} \ , \end{aligned} \tag{5}$$

where the function γ is a generalized Dirac function,

$$\gamma_n(r_1,r_2,\ldots,r_m)=\begin{cases}1 \text{ if } \sum_{i=1}^{m} r_i=n \ , \\ 0 \text{ otherwise} \ .\end{cases} \tag{6}$$

The first summation in (5) encompasses all different combinations of r_i, excluding possible permuatations.

For a chain of N spins $\mathrm{tr}(\mathcal{H}_N^n)$ may be expressed in the $D(n)$'s and $d(n)$'s

$$\mathrm{tr}(\mathcal{H}_N^n)=\sum_{k=1}^{\alpha_n} Q_{\vec{\Gamma}_k}^N D_{\vec{\Gamma}_k}(n)+\sum_{l=1}^{\beta_n} q_l^N d_l(n) \ , \tag{7}$$

with Q_k^N indicating the occurrence of graph $D_{\vec{\Gamma}_k}(n)$ on a chain of N spins and α_n for the number of different composite graphs of the order n (and corresponding definitions for q_l^N and β_n).

In order to calculate a coefficient in the series expansion for the infinite chain (3) by the moment method, one must calculate the trace of each graph that may contribute to the corresponding order, multiplied by the coefficient of the linear term in its occurrence function (e.g., Rushbrooke and Wood[20]). The occurrence of each simple graph is, in our definition, just once per site for the infinite chain. For composite graphs, $Q_{\vec{\Gamma}}^N$ also contains terms in N^2, N^3, etc. If we denote the term proportional to N in $Q_{\vec{\Gamma}}^N$ by $\eta_{\vec{\Gamma}}$ then the coefficients a_i in (3) are found from

$$a_n=\frac{2^n}{n!}\left(\sum_{l=1}^{\beta_n} d_l(n)+\sum_{k=1}^{\alpha_n}\eta_{\vec{\Gamma}_k} D_{\vec{\Gamma}_k}(n)\right) . \tag{8}$$

Since, according to (5), the trace of a composite graph may be expressed in products of the traces of its composing simple graphs, it is sufficient

to know all $d_l(m)$ with $m<n$ in order to calculate a_n. But Eq. (7) shows that $\mathrm{tr}(\mathcal{K}_N^n)$ can also be expressed in $d_l(m)$ with $m<n$, and it should therefore be possible to relate a_n to $\mathrm{tr}(\mathcal{K}_N^n)$ for different N. Instead of establishing this relationship directly we shall content ourselves with the solution of all $d_l(n)$ and then substitute them in (8).

B. Calculation of $d_l(n)$

The calculation of the trace of a graph $d_l(n)$ is most simply formulated with an induction formalism. Suppose that the value associated with all $d_l(m)$ is known for all $m<n$. Since a composite graph of the order n is composed of simple graphs of orders smaller than n, all $D\mathfrak{T}(n)$ may be calculated according to (5). Then Eq. (7) can be rewritten as a set of linear equations with $d_l(n)$ unknown:

$$\tilde{\mathbf{q}}\,\vec{\mathbf{d}}(n) = \vec{\mathbf{B}}(n) \ , \tag{9}$$

where the components of $\vec{\mathbf{B}}(n)$ are related with the Hamiltonian for different chains as

$$B_N(n) = \mathrm{tr}(\mathcal{K}_N^n) - \sum_{k=1}^{\alpha_n} Q_{\mathfrak{T}_k}^N D\mathfrak{T}_k(n) \ . \tag{10}$$

The number of equations equals the number of chain lengths for which $\mathrm{tr}(\mathcal{K}_N^n)$ could be calculated and the number of unknowns is β_n. This set of equations may be solved as long as no two simple graphs have all q^N equal. This requirement is satisfied since the lengths of two simple graphs is unequal, and $q_l^N = N-l+1$ for chains. A unique solution is then found if β_n is at most equal to the number of chains. Owing to the fact that $\mathrm{tr}(\vec{\mathbf{S}}_i \cdot \vec{\mathbf{S}}_{i+1})$ vanishes, β_n is found to be

$$\beta_n = \begin{cases} \frac{1}{2}n, & n \text{ even} \\ \frac{1}{2}(n-1), & n \text{ odd} \ . \end{cases} \tag{11}$$

Therefore, the contribution of all $d_l(n)$ can be calculated for $n<2N-1$ when $\mathrm{tr}(\mathcal{K}_L^n)$ is known for all $L<N$.

Returning to the original calculation we note that once $d_l(m)$ is known for all $m<n$, $d_l(n)$ could be calculated. Since $d_1(2)$ [the smallest order with nonvanishing $d(m)$] is known, all $d(m)$ can therefore be found.

The method so far has not distinguished between rings and chains, except for the actual values of the occurrence functions. However, when $\mathrm{tr}(\mathcal{K}_N^n)$ is calculated for a ring of N spins there will be a contribution of a polygon $P_N(n)$ (ring graph) if $n \geq N$. This introduces additional unknowns in Eq. (9). Since it is difficult to correlate polygons of different length, the use of rings is limited to $n<N$. Although rings have higher symmetry and should therefore be solvable with more spins than is possible for a chain, their application to this technique is limited. However, owing to the periodicity of a ring, the thermodynamic functions, when normalized per spin, are correct to the order $n=N-1$. This will be a useful check in the calculations.

The important question about any systematic error in the theory or in the actual numerical computation of the graphs was examined with great care. First of all we recall the set up of the calculation. The method outlined was one of complete induction and the computer programming was correspondingly a recursive algorithm. This actually leads to one of the few cases in which the correctness of a program can be proved.[33] The calculation of the occurrence functions q_l^N and $Q_{\mathfrak{T}}^N$ is elementary in this case and yields no particular difficulties. All further steps in the calculation of a_n were checked by comparison with the results of direct calculation of the first ten terms in the series, following the general outline of Rushbrooke and Wood.[20] The propagation of rounding errors in the stepwise calculation of $d(n)$ might cause trouble. Except for the highest order, the set of equations (9) is overdetermined. The solution is then found using a least-squares criterion, and the squares' sum is a reliable measure of the correctness of the results. Since of all $d_l(n)$ for a certain order n, $d_1(n)$ has always the smallest value, any rounding errors will affect this graph most clearly. In the Appendix it is shown how $d_1(n)$ can be calculated exactly from first principles, and this provides a check on the influence of the propagation of errors. Finally, we note that the cumulant method independently leads to the same coefficients a_n, and a comparison between the two results again serves as a check (see Sec. III C).

As we mentioned in the introduction to this section, one further coefficient in the series (3) can be calculated approximatively. This additional term requires knowledge of the contribution of all graphs in $\mathrm{tr}(\mathcal{K}_L^{2L})$, where L is the number of spins in the longest chain that was solved. Examination of Eqs. (8)–(10) shows that any $d_l(2L)$ can be solved except those with $l>L-1$. This leaves only one graph to be calculated, $d_L(2L)$, which consists of a double bar between $L+1$ consecutive sites. An approximate solution is possible owing to its relative simplicity. This can best be demonstrated by starting with $d_2(4)$ and examining the different terms that make up this graph:

$$d_2(4) = 4T_{1,2} + 2R_{1,2} \ , \tag{12}$$

with

$$T_{i,i+1} = (\vec{S}_i \cdot \vec{S}_{i+1})(\vec{S}_i \cdot \vec{S}_{i+1})(\vec{S}_{i+1} \cdot \vec{S}_{i+2})(\vec{S}_{i+1} \cdot \vec{S}_{i+2}) \tag{13a}$$

and

$$R_{i,i+1} = (\vec{S}_i \cdot \vec{S}_{i+1})(\vec{S}_{i+1} \cdot \vec{S}_{i+2})(\vec{S}_i \cdot \vec{S}_{i+1})(\vec{S}_{i+1} \cdot \vec{S}_{i+2}) \,. \tag{13b}$$

In general the terms T and R have different values. They are a basis for the two groups of different permutations of four quantities belonging to two groups of two. Now for $d_3(6)$ there will be combinations of $T_{1,2}$, $R_{1,2}$, $T_{2,3}$, and $R_{2,3}$. Here again $T_{1,2}$ occurs twice as often as $R_{1,2}$ as is also the case with $T_{2,3}$ relative to $R_{2,3}$, and the total number adds up to $6!/(2!)^3$.

Tentatively, therefore, one might express $d_3(6)$ in $d_2(4)$ as

$$d_3(6) = \tfrac{1}{6} d_2(4)(4T_{2,3} + 2R_{2,3})\, 6!/(4!\,2!) \,, \tag{14}$$

or for general order

$$d_{l+1}(2l+2) = \tfrac{1}{6} d_l(2l)(4T + 2R)(2l+1)(2l+2)/2 \,, \tag{15}$$

where the subscripts to T and R are omitted since they do not affect their respective values. Both formulas are incorrect since it was assumed that T and R occur four times and twice, respectively, irrespective of the terms already present in the smaller graph. Actually there are correlations between these terms, as can be verified from Table II where we list the possible combinations for $d_3(6)$. For a large number of terms, as in the case of $d_{11}(22)$ for $S = \frac{1}{2}$, one may assume that there will be a more or less constant distribution over all terms and then Eq. (15) may be generalized to

$$d_{l+1}(2l+2) = d_l(2l)\alpha(2l+1)(2l+2) \,, \tag{16}$$

with α a constant.

A plot of $d_{l+1}(2l+2)/d_l(2l)$ against $(2l+1)(2l+2)$ would thus show linear behavior. The results for $S = \frac{1}{2}$ are plotted in this way in Fig. 1 and it is obvious that Eq. (16) is a good approximation. The approximate value of $d_{11}(22)$ for $S = \frac{1}{2}$ can be calculated in this way and is accurate within 0.1%. This results in a possible relative error of 10^{-7} in the coefficient a_{22}. Similar calculations were performed for the case of other S, although the errors increase considerably with increasing S. The resulting errors are summarized when the series are presented in full detail in Sec. III D.

TABLE II. Trace of the graph $d_3(6)$ has contributions from terms with different symmetry. The occurrence of combinations of these terms is listed together with the numbers that result if these terms are assumed to be independent.

Term pair	Real occurrence	Estimate of Eq. (14)
$T_{12}\,T_{23}$	42	40
$T_{12}\,R_{23}$	18	20
$R_{12}\,T_{23}$	18	20
$R_{12}\,R_{23}$	12	10

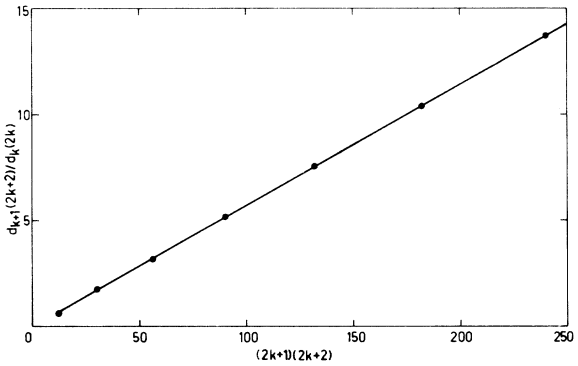

FIG. 1. Plot of $d_{k+1}(2k+2)/d_k(2k)$ vs $(2k+1)(2k+2)$ for $S = \frac{1}{2}$. The asymptotic linear behavior is used in order to estimate an additional coefficient in the HTE.

First, the cumulant method of obtaining the coefficients will be outlined.

C. Cumulant method

Instead of expanding the partition function, an expansion of $\ln(Z)$ or the Gibbs free energy is possible also. An important consequence of such an expansion is that only simple graphs are of importance,[30] which introduces a great simplification into the calculation. Especially for a higher lattice dimensionality the enumeration of the occurrence functions for composite graphs Q_Γ^N is complicated. For a 1-d lattice there is little reason to favor one method over the other, and we merely used them both as a partly independent check.

Following the outline of Rushbrooke,[30] we may specialize the method for chains and express the specific heat per site for different chains (C_n) in the cumulant functions Φ_i as

$$\begin{aligned} C_1 &= \Phi_1 \,, \\ 2C_2 &= 2\Phi_1 + \Phi_2 \,, \\ 3C_3 &= 3\Phi_1 + 2\Phi_2 + \Phi_3 \,. \end{aligned} \tag{17}$$

For general chain length we then obtain the analog of Eq. (7):

$$NC_N = \sum_{k=1}^{N} q_k^N \Phi_k = \sum_{k=1}^{N} (N-k+1)\,\Phi_k \,. \tag{18}$$

The cumulant functions Φ_i are, like the specific heat, functions of temperature. Each can be expressed in a power series in β

$$\Phi_k = \sum_{i \geq 2k} c_{ki} \beta^i \ , \tag{19a}$$

$$C_k = \frac{1}{k} \sum d_{ki} \beta^i \ , \tag{19b}$$

and the important observation is (e.g., Rushbrooke *et al.*[34]) that $c_{ki} = 0$ for $i < 2k$. The coefficients c_{ki} may be solved stepwise, according to Eq. (17), i.e., first all c_{1i} in Φ_1, which equal the coefficients in the expansion of C_1, then c_{2i} by examining $2(C_2 - \Phi_1)$, etc. However, this would result in unnecessary error propagation and it is therefore better to use the analog of Eq. (9), and solve the c_{ki} from

$$\vec{\mathsf{q}}\,\vec{c} = \vec{d}_k \ . \tag{20}$$

In this way one obtains, except for the highest order, an overdetermined set of equations which can be solved in the sense of a least-squares fit. Generally this is sufficient to obtain numerical stability.

D. Results of the series expansions

The moment method and the cumulant method both make use of the eigenvalues of the Hamiltonians for finite chains. The results are therefore not completely independent, nor even their errors. We note that a higher degree of accuracy may be obtained when the traces $\mathrm{tr}(\mathcal{H}^n)$ are calculated directly by repeated multiplication of the matrix representation of $\mathcal{H}$ by itself and then summing the diagonal elements. Since we started with a calculation of the eigenvalues in order to obtain the thermodynamic behavior of finite chains, we did not employ this technique but used the eigenvalues as the basic entities. Besides for $S \neq \frac{1}{2}$ the matrix of $\mathcal{H}$ contains square roots of integer numbers and a complete integer arithmetic is thus not possible anyhow.

The way of solving the traces of simple graphs and cumulant functions with a least-squares criterion gives, except for the highest coefficients, an indication of their errors. Very surprisingly, this suggests that the errors in the coefficients obtained by the cumulant method are about three orders of magnitude higher than those from the moment method, although the latter involves more complicated steps. Apparently an error in $d_l(k)$,

TABLE III. Coefficients in the series expansion of the specific heat of an $S = \frac{1}{2}$ chain, $C = \frac{3}{4}\beta^2 J^2 \sum_{i \geq 0} b_i (\frac{3}{4}\beta J)^i$.

i	b_i
0	1.0
1	−1.333 333
2	−2.222 222
3	5.925 926
4	1.382 716
5	−16.100 960
6	8.293 370
7	31.980 259
8	−41.425 570
9	−43.403 537
10	121.959 798
11	11.991 318
12	−273.767 213
13	159.718 026
14	479.797 98
15	−664.302 69
16	572.727 27
17	1798.4461
18	1827.128
19	−12 696.13
20	−100 357.5

TABLE IV. Coefficients in the HTE of the specific heat of an $S = 1$ chain, $C = \frac{16}{3}\beta^2 J^2 \sum_{i \geq 0} b_i (2\beta J)^i$.

i	b_i
0	1.0
1	−0.5
2	−1.666 666
3	1.250 000
4	2.138 889
5	−2.226 389
6	−2.397 016
7	3.447 366
8	2.364 325
9	−4.902 016
10	−1.939 088
11	6.541 397
12	1.35 ± 0.2

TABLE V. Coefficients in the HTE of the specific heat of an $S = \frac{3}{2}$ chain, $C = \frac{75}{4}\beta^2 J^2 \sum_{i \geq 0} b_i (\frac{15}{4}\beta J)^i$.

i	b_i
0	1.0
1	−0.266 667
2	−1.312 000
3	0.477 234
4	1.355 578
5	−0.625 065
6	−1.279 653
7	0.726 823
8	1.148 911
9	−0.791 381
10	−1.07 ± 0.02

TABLE VI. Coefficients in the HTE of the specific heat of an $S=2$ chain, $C=48\beta^2J^2\sum_{i\geq 0} b_i(6\beta J)^i$.

i	b_i
0	1.0
1	−0.166667
2	−1.133333
3	0.243827
4	1.009671
5	−0.267781
6	−0.823004
7	0.262774
8	0.57 ±0.06

through the action of composite graphs to which it contributes, does stablilze the errors in subsequent coefficients.

The series coefficients, as we present them in Tables III–VII, are rounded off to six decimals, except for the final ones in each series. Our checks indicate this to be the correct number of reliable digits for the higher coefficients. The last coefficient in each series, found by application of Eq. (16), is very rough for higher spin. The errors are indicated in the tables. In order to obtain coefficients of the order of unity, the series are expressed in powers of $J\beta S(S+1)$ instead of $J\beta$.

IV. INTERMEDIATE-TEMPERATURE REGION

As is well known, a 1-d arrangement of spins with short-range interactions cannot sustain a state of long-range order and instead of a singularity in C, a broad maximum is observed. The results obtained through direct application of the HTE do not even indicate such a broad maximum, as shown in Fig. 2. Therefore, in the neighborhood of this maximum ($T\simeq S^2J$) other techniques have to be used. The analysis of the series coefficients by Padé approximants (PA) has been

TABLE VII. Coefficients in the HTE of the specific heat of an $S=\frac{5}{2}$ chain, $C=\frac{1225}{12}\beta^2J^2\sum_{i\geq 0} b_i(\frac{35}{4}\beta J)^i$.

i	b_i
0	1.0
1	−0.114286
2	−0.103336
3	0.147032
4	0.838068
5	−0.145777
6	−0.619784
7	0.129303
8	1.5 ±0.3

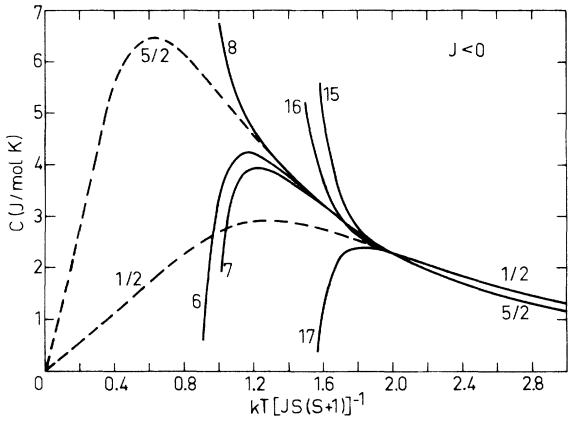

FIG. 2. Antiferromagnetic specific heat as a function of reduced temperature $T^*=kT/JS(S+1)$, for $S=\frac{1}{2}$ and $S=\frac{5}{2}$. The curves represent estimates based on a finite number of terms in the HTE. The numbers indicate the power of β in the last term of the series.

shown to increase the region of usefulness of a series considerably.[29] Basically, a PA indicates the position of poles in the complex β plane, which determine the convergence radius of the HTE, and the removal of these poles from the series automatically extends its applicability.

A very brief description of the method and the presentation of results obtained in this way is given in Sec. IV A. A more direct approach to the PA, possible in the case of chains, is discussed also.

The special structure of the equations used in the calculation of the HTE coefficients, especially the simple form of the occurrence functions q_l^N, enables a direct relation between the specific heat per site in chains of different length to be established. The use of this relation automatically leads to a simple extrapolation of the results to the case $N\to\infty$. In Sec. IV B this technique will be outlined, and it will be shown that the results obtained in this way are reliable in the high-temperature region and in the intermediate-temperature range.

A. Padé approximants

The construction of a Padé approximant $[N/D]$ as a quotient of two polynomials of the orders N and D, of which the series expansion equals that of a given series to the order $N+D$ has been well established by the studies of Baker[35] and others.[36]

It is convenient to apply the PA to the logarithmic derivative of the specific-heat series, assuming a power-law divergence of C. Since in our case of a 1-d lattice no long-range order can exist, the singularities in C will lie in the complex

β plane, off the real axis. The series of C may then be written in the form

$$C = \frac{\sum_i b_i \beta^i}{(\beta - \beta_0)^\gamma (\beta - \beta_0^*)^{\gamma *}} , \quad (21)$$

where β_0 and β_0^* indicate the position of the two conjugated poles closest to the origin. The order of the poles are γ and γ^*, respectively, ensuring a real expression for real β. The zeros of the denominator of a PA to $(\partial C/\partial\beta)/C$ then indicate the position of β_0 and β_0^* and the residue of the PA in β_0 is a measure of γ.

When β_0 and γ settle around a limiting value for different $[N/D]$, we may obtain the specific heat by direct integration of the $[N/D]$ and expect that the result will not vary much when changing N and D. On the other hand it is possible also to average over the different β_0 and γ found from various $[N/D]$ and construct a new series for C according to Eq. (21). In this latter case the region of reliable application can be found as in the case of the original HTE by constructing the curves resulting from (21) with a varying number of terms in the nominator.

The results thus obtained are not very convincing. First of all the temperature region of reliable application is not as large as was hoped. Secondly, we find a residue γ which is spin dependent. For $S = \frac{1}{2}$, $\gamma = 1.55 \pm 0.01$ and for $S = \frac{5}{2}$, $\gamma = 1.83 \pm 0.05$. Such spin dependence does not fit in with the general assumptions of universality.[9,37]

In order to examine the poles more closely, we turned to the following simple consideration. Since C is a derivative of the Gibbs free energy G, any pole in C may be caused by a zero in the partition function Z. We can thus study the zeros of Z for different chains and so estimate their limiting behavior. Figure 3 displays the position of these zeros for a number of chain lengths when $S = \frac{1}{2}$. Since the location of roots of a complex function is not at all simple, we did not attempt to find them all, but those shown in the plot are sufficient to give an idea of the behavior. With increasing chain length, the number of roots increases and their location changes. The lines indicate this change of position. Several lines can thus be drawn, all approaching the point $\beta_0 = -0.11 \pm 0.46i$ obtained from the PA analysis. All zeros lead to a residue $\gamma = 2$, since, if we write

$$Z = (\beta - \beta_0)^\delta (\beta - \beta_0^*)^{\delta *} \theta(\beta) , \quad (22)$$

then

$$C = \frac{\delta\beta^2}{(\beta - \beta_0)^2} + \frac{\delta^*\beta^2}{(\beta - \beta_0^*)^2} + \frac{\beta^2}{\theta^2}[\theta\theta'' - (\theta')^2] . \quad (23)$$

It is hard to justify the conclusion that $\gamma = 2$ in the limit $N \to \infty$ since several poles, distinct for finite N, then coincide. We found, however, that for $\gamma = 2$, a β_0 can be located such that in (21) all b_i with $i > 2$ become of the order of 0.1 (while in the original series the highest coefficients are of the order of 20). We also note that an approximate fitting of the estimated C for $N \to \infty$ results in $\gamma \simeq 2$ for all S as was shown in a preliminary paper.[38] See also Sec. VI.

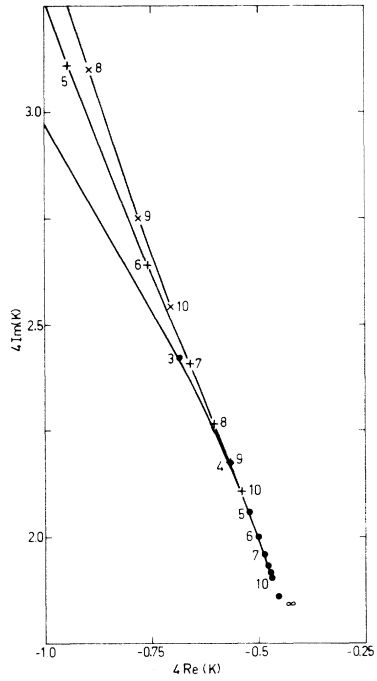

FIG. 3. Position of some roots in the partition function for finite chains, together with the estimated limit for the infinite chain. The numbers indicate the length of the chains. Only those roots are shown that display a regular behavior for increasing number of spins. Others exist but are generally further from the origin.

The uncertainty in γ may be related to the fact that the usefulness of an HTE generally increases with increasing coordination number of the lattice (see, for instance, the difference between two- and three-dimensional lattices[39,40] and, for 3-d systems, the difference between open- and close-packed arrangements[35]). One may anticipate that in the case of a 1-d lattice this situation will be worst and that therefore the results of a PA analysis of such series should be interpreted with care.

Fortunately we are not primarily interested in the order of the singularities but in an estimate of C for real temperatures. It has been shown that direct extrapolation of the results for different chain lengths to the limit $N \to \infty$ is possible and that such a procedure results in fairly reliable estimates for a wide range of temperatures. In a

previous paper[38] the basis of this technique was derived from an examination of the HTE. A more rigorous foundation was found afterwards and will be presented in Sec. IV B.

B. Direct extrapolation of finite chains

The simplicity of Eq. (18) offers a basis for a direct relation between the specific heat per site in finite and infinite chains. Rearranging the terms in (18) readily leads to the relation

$$C_N = C_\infty - \frac{b}{N} + \frac{1}{N}\sum_{k=1}^{\infty} k\Phi_{k+N+1}\,, \tag{24}$$

where

$$b = \sum_{k=1}^{\infty} (k-1)\Phi_k \tag{25}$$

is independent of N. Since the cumulant function Φ_k is a polynomial in β starting with β^{2k-2},[34] we may thus write

$$C_N = C_\infty - b/N + O(\beta^{2N+2})\,. \tag{26}$$

That is, for sufficiently high temperatures, C_∞ may be obtained from a plot of C_N against $1/N$ for a given temperature. Increasing β will result in deviations from the supposed linear relation between C_N and $1/N$ and this is indicated in Fig. 4 where C_N is plotted for two temperatures. Obviously the correction term $O(\beta^{2N+2})$ has an alternating effect in accordance with N even and odd. This offers a good possibility of extrapolation. Using a least-squares criterion, C_∞ and b may be calculated so as to fit in best with the plotted C_N for any temperature. A higher weight may be assigned to the points for high N but this is not necessary. In any case the squares's sum offers a reliable measure of the error in the estimate of C_∞.

The procedure outlined gives good results by itself for $S=\frac{1}{2}$ and $S=1$. Figure 5 shows the estimates obtained in this way for these two cases and a comparison with Fig. 2 marks the extension of the useful temperature range compared with the results from the HTE.

For higher spin, and especially for $S=\frac{5}{2}$, where the longest chain has $N=5$ only, the estimates are based on a smaller number of points. But still, this procedure gives fair results. To understand this, one may observe that for $S\to\infty$, $C_N = NC_\infty/(N-1)$ is exact for all $N>1$. For higher spin the deviations from (26) are therefore smaller and this compensates the loss of data points in constructions as in Fig. 4.

When rings are used as the basic items for an extrapolation procedure, we may rederive Eq. (25). If the cumulant function associated with a polygon of N spins is denoted by ϕ_N, we may write

$$C_N^{\text{ring}} = C_\infty - \frac{1}{N}\sum_{k=0}^{\infty}\Phi_{N+k} + \frac{\phi_N}{N}\,. \tag{27}$$

In this way the correction term is $O(\beta^N)$. In comparison with the chain formula this is a loss of $O(\beta^{N+2})$. But a more important restriction is found in the behavior of the last term in Eq. (27). For antiferromagnetic exchange this term is alternating in sign for different N but for ferromagnetic coupling the term is of uniform sign. This

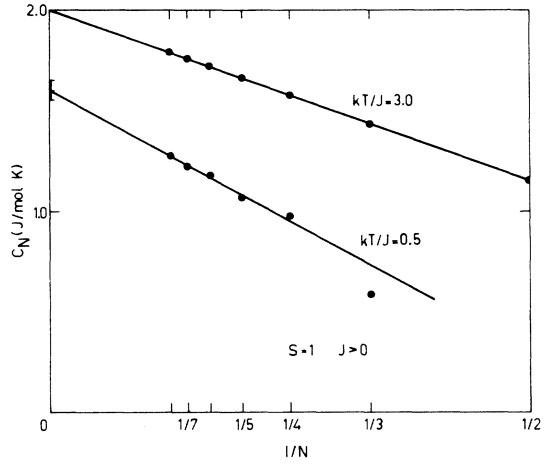

FIG. 4. A plot of C_N vs $1/N$ for $S=1$ chains. At high temperatures the data points obey a linear relation. At lower temperatures deviations from this linearity are observed. The error bar in this last case indicates an interval of 2σ where σ is the standard deviation.

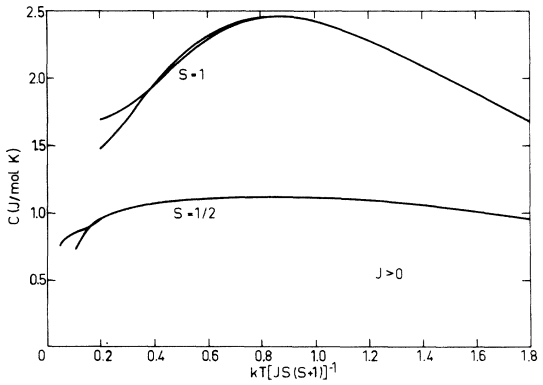

FIG. 5. Estimates of the specific heat of an infinite ferromagnetic chain for $S=\frac{1}{2}$ and $S=1$. The estimates are obtained from a direct extrapolation of C_N vs $1/N$ (cf. Fig. 4). The two curves shown for each S deviate in the low-temperature region and indicate the uncertainty of the result.

severely limits the temperature range of application as may be seen from the work of Bonner and Fisher.[15] These authors already pointed out the similarity between the specific-heat curves for different (short) *chains*. It is this similarity that actually leads to the sound procedure outlined in this section.

V. LOW-TEMPERATURE REGION

When the energy spectrum of a finite ring or chain is known, one may construct a density function of the energy levels. On examination of this function for clusters of different size one may note a gradual steadying of its shape with increasing cluster size. That is, after smoothing, the difference between the functions for chains with N and with $N-1$ spins decrease with increasing N. This is indicative of the possibility of constructing a limiting function and hence proceeding to an estimate of the thermodynamic functions in that limit. The discussion of the last two sections showed this to be true for sufficiently high temperatures. On closer examination, however, the differences will be more marked. It is thus very hard to use information on finite systems in cases where the details of the density function are essential.

This obviously excludes the low-temperature region, where only a few energy levels are of importance and dominate the thermodynamic behavior. Nevertheless it was shown by Bonner and Fisher[15] that reasonable estimates may be obtained since the ratio of certain quantities is less sensitive to the deviations in the energy spectrum than the quantities themselves. For instance, a plot of internal energy U against the product of temperature and entropy (to exclude confusion, η will be used for this quantity instead of S) shows a linear relation down to fairly low temperatures. And if one assumes a power law behavior for U near $T=0$, viz.,

$$U(T) - U(0) = AJT^{\alpha}, \tag{28}$$

then obviously

$$U(T) - U(0) = (1 - 1/\alpha)\, T\eta(T), \tag{29}$$

which explains the linearity. Moreover, the exponent α may be found from such a plot. The amplitude A can then be determined otherwise and the results used to obtain the specific heat in the very-low-temperature region.

The description of $C(T)$ near $T=0$ found in this way compares with the prediction of spin-wave theory[26] in the sense that the exponent $\alpha = \frac{3}{2}$ for $J>0$ and $\alpha = 2$ for $J<0$. Discrepancies exist however in the magnitude of A (cf. Weng for $S=1$).[21] Green's-function analysis[23] (GFA) also predicts the values for α mentioned; the amplitude is found very close to the U vs. $T\eta$ results. This analysis, moreover, indicates that the region in which (28) may be assumed is small.

In our examination of the low-temperature behavior we started from the assumption (28) and checked whether α was spin independent using plots of U vs $T\eta$. This was found to be the case. In order to find a reasonable estimate of $C(T)$ in this region, noting the prediction of the GFA, we attempted to describe $C(T)$ by a polynomial in T. For ferromagnetic exchange, for instance, we assumed

$$C(T) = a_1(kT/J)^{1/2} + a_2(kT/J)^{3/2} + a_3(kT/J)^{5/2} \tag{30}$$

and equated the coefficients such that at a certain

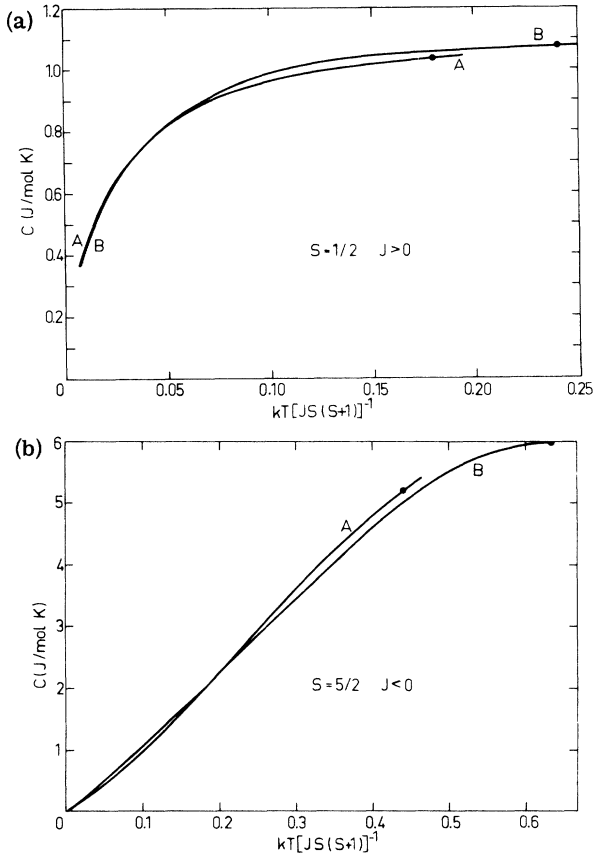

FIG. 6. (a) Low-temperature specific heat of a ferromagnetic chain with $S=\frac{1}{2}$. The two curves are obtained by equating the coefficients in the assumed polynomial such that the curves fit in smoothly with the estimated C at different temperatures. The curves have been drawn below the corresponding take-over temperature. (b) Low-temperature specific heat for $S=\frac{5}{2}$, $J<0$. The comment of Fig. 6(a) applies here also.

temperature T_0 the curve fits in with the estimate obtained by direct extrapolation (cf. Sec. IV) both in value and in slope. Moreover, it is required that the total entropy gain between $T=0$ and $T\to\infty$ equals $R\ln(2S+1)$. If the expression (30) is reasonably good, little influence is expected from a change of T_0.

Figure 6(a) shows the influence of T_0 for the ferromagnetic chain with $S=\frac{1}{2}$. The different curves have been drawn in the interval $0<T<T_0$, and although discrepancies are present the maximum deviation does not exceed 3%. Curve A results when $kT_0/J=0.24$, which is about the lowest temperature at which the intermediate-temperature extrapolation is reliable. For a 30% higher value of T_0, curve B was obtained. Solutions for $0.24<kT_0/J<0.32$ show an array of curves that lie between the two drawn. In view of the considerable difference between $T_0(A)$ and $T_0(B)$, the maximum deviation of 3% between the two results is not surprising. In case of antiferromagnetic exchange the leading term should be in T and the polynomial used then reads

$$C(T)=b_1|kT/J|+b_2|kT/J|^2+b_3|kT/J|^3\ . \qquad (31)$$

In this case too, the resulting curves are quite insensitive to the value of T_0, and deviations like those shown in Fig. 6(b) are representative. The actual values of the coefficients are tabulated in Tables VIII and IX.

It should be noted that an additional coefficient may be introduced if the internal energy gain $U(\infty)-U(0)$ is also required to be correct. However, the result is not sensitive to this requirement since $U(0)-U(T_0)$ is very small for the T_0 we have used.

The description of the low-temperature part of the specific heat by polynomials as introduced above is based on spin-wave theory, so one might expect it to be at least qualitatively correct. In a way the insensitivity of the resulting curves to changes in T_0 is an indication of this. Nevertheless, there are considerable differences in the numerical result as compared to spin-wave and GFA predictions and extrapolation from rings.[15]

The coefficients of the leading terms in the series (30) and (31) are compared for various techniques in Tables X and XI. In these tables the coefficients correspond to C/R in order to simplify comparison with published work. We note that in the case of ferromagnetic exchange the predictions from the various techniques do not differ much. For antiferromagnetic exchange, however, large discrepancies are observed. In this case we can refer to some theoretical results for the $S=\frac{1}{2}$ chain. The leading term in (31) was calculated as $b_1/R=\frac{1}{3}$,[43-45] as a special case of a general expression for the axial Hamiltonian. Examination of Table XI shows that spin-wave theory[42] predicts unreasonably high values, while our own results are low compared to similar work of Bonner and Fisher[15] and Weng.[21] In comparing our predicted specific-heat curve with that of Bonner and Fisher, we note excellent agreement for all temperatures above $kT/J=0.3$. For lower temperatures our result is systematically lower with a maximum difference of about 70%. Since the difference in entropy gain is only 2%, which is accounted for in both our uncertainty in η at T_0 and Bonner and Fisher's over-all uncertainty, it must be concluded that differences of this order

TABLE VIII. Coefficients in the polynomial used for the description of the low-temperature specific heat of ferromagnetic chains, $C=a_1(kT/J)^{1/2}+a_2(kT/J)^{3/2}+a_3(kT/J)^{5/2}$. T_0^* is the reduced temperature $kT_0/JS(S+1)$ where this polynomial is fitted in with the estimated C in the intermediate-temperature region.

	$S=\frac{1}{2}$	$S=1$	$S=\frac{3}{2}$	$S=1$	$S=\frac{5}{2}$
a_1	3.77	2.81	2.45	2.01	1.91
a_2	−9.96	−1.20	−0.73	0.06	−0.09
a_3	12.99	0.56	0.39	0.001	0.04
T_0^*	0.2125	0.45	0.325	0.425	0.325

TABLE IX. Coefficients in the polynomial used for the description of the low-temperature specific heat of antiferromagnetic chains, $C=b_1|kT/J|+b_2|kT/J|^2+b_3|kT/J|^3$. The take-over temperature T_0^* is in conformity with the description in Table VIII.

	$S=\frac{1}{2}$	$S=1$	$S=\frac{3}{2}$	$S=2$	$S=\frac{5}{2}$
b_1	1.67	0.90	1.02	1.27	1.15
b_2	7.10	4.60	2.05	0.71	0.41
b_3	−6.04	−2.16	−0.68	−0.17	−0.08
T_0^*	0.8	0.7	0.4	0.475	0.4

TABLE X. Comparison of predictions for the coefficient of $T^{1/2}$ in the expression for C/k near $T=0$ in case of ferromagnetic coupling: BF, Bonner and Fisher (Ref. 15); RS, Rhodes and Scales (Ref. 23); SW, spin-wave theory (cf. Keffer, Ref. 26); W, Weng (Ref. 21); deN, this work.

$J>0$	$S=\frac{1}{2}$	$S=1$	$S=\frac{3}{2}$	$S=2$	$S=\frac{5}{2}$
BF	0.42				
RS	0.46	0.424	0.379	0.340	0.307
SW	0.552	0.391	0.319	0.276	0.247
W		0.297			
deN	0.45	0.338	0.295	0.242	0.230

TABLE XI. Comparison of predictions for the coefficient of T in the expression for C/k near $T=0$ in case of antiferromagnetic exchange: BF, Bonner and Fisher (Ref. 15); KY, Kondo and Yamaji (Ref. 41); SW, spin-wave theory (cf. Kubo, Ref. 42); W, Weng (Ref. 21); deN, this work.

$J<0$	$S=\frac{1}{2}$	$S=1$	$S=\frac{3}{2}$	$S=2$	$S=\frac{5}{2}$
BF	0.35				
KY	<0.05				
SW	1.047	0.523	0.349	0.262	0.209
W		0.4			
deN	0.200	0.108	0.123	0.153	0.138

are not unaccountable in the extreme-low-temperature region. The differences in entropy gain between Weng's estimate and ours for $S=1$ are larger. We think it likely that Weng's total entropy gain it too high by about 6%.

In order to estimate the ground-state energy for the infinite antiferromagnetic chain, a plot of $U_N(0)$ against some inverse power of N was shown to be useful.

For $S=\frac{1}{2}$ Bonner and Fisher[15] used N^{-2}, and N^{-3} was used by Weng[21] for $S=1$. Weng pointed out that since for $S\to\infty$, $U_N(0)$ against $N^{-(2S+1)}$ would result in a straight line for general S. Our data do not support this prediction. First of all the results for $S=1$ may hardly be said to obey the relation

$$U_N(0) = U_\infty(0) + \alpha/N^K \tag{32}$$

with $K=3$ [for details of $U_N(0)$ for different N and S see Table XII]. Secondly, the data for $S=\frac{3}{2}$ cannot be fitted in with an equation of the form (32) at all.

For $S>\frac{3}{2}$ not enough data points are available to examine the relation. The technique as used by Duffy and Barr[46] is not possible either, for the same reason.

TABLE XII. Ground-state energy E_0/NJ for antiferromagnetic rings of different size. The row with $N=\infty$ indicates the lower bound for E_0/NJ based on Eq. (34) for the infinite ring or chain.

N	$S=\frac{1}{2}$	$S=1$	$S=\frac{3}{2}$	$S=2$	$S=\frac{5}{2}$
3	0.5	2.0	3.5	6.0	8.5
4	1.0	3.0	6.0	10.0	15.0
5	0.747	2.612	4.972	8.456	12.426
6	0.934	2.872	5.796		
7	0.816	2.734			
8	0.913	2.834			
9	0.844				
10	0.903				
11	0.858				
12	0.898				
13	0.866				
∞	0.833	2.857	5.900	9.935	14.960

The results for the low spin values ($S<\frac{3}{2}$) indicate that in all cases a prediction of $U_\infty(0)$ based on the connection of $U_N(0)$ and $U_{N+2}(0)$ in a plot of $U_K(0)$ against $K^{-(2S+1)}$ results in a value that is too negative when the data of even-numbered rings are used. [It may hardly be expected that odd numbered rings obey a relation like (32) since for $S\to\infty$ the ground-state energy is proportional to $\cos(2\pi/N)$.] If such behavior is assumed for all S, then clearly (32) may be used to obtain a lower bound for $U_\infty(0)$. With the aid of the exact results for rings with $N=2$ and $N=4$ (Appendix) we then arrive at the relation

$$U_\infty(0) > [2S^2 + S(2^\kappa - 2)/(2^\kappa - 1)]J \tag{33}$$

with $\kappa = 2S+1$, and $J<0$.

The lower bounds obtained in this way are summarized in Table XII together with the estimates available for small S.

VI. DISCUSSION OF THE RESULTS

Fragments of the results were shown in the preceding paragraphs. Here we shall present and discuss the estimates for the thermodynamic behavior of the infinite chain, resulting from a combination of the different techniques that were used.

For antiferromagnetic interaction a combination of high-, low-, and intermediate-temperature techniques results in the curves shown in Figs. 7 and 8 for C and η, respectively. The specific heat has always been our basic quantity in all three temperature regions (for the series expansion around $\beta=0$, for the direct extrapolation to $N\to\infty$ in the neighborhood of $C_{\max}$ and for the fitting around $T=0$). The entropy is obtained by integration of C/T. The requirements made upon the evaluation of the coefficients in the low-temperature polynomial guarantee the correct over-all entropy gain of $R\ln(2S+1)$ between $T=0$ and $T\to\infty$.

As could be expected, C increases monotonically with increasing spin when scaled to a reduced temperature $T^*=kT/JS(S+1)$, and the reduced temperature for which C attains its maximum value (T_m^*) gradually decreases. In the limit $S\to\infty$, T_m^* tends to zero.

The take-over temperatures T_0, where the low-temperature polynomials are fitted in with the estimated curves obtained from direct extrapolations of finite chains, are indicated in Fig. 7. The scatter of these points is due to the differences in the estimated uncertainty of the results from the direct extrapolations. Although the maximum chain length for which the eigenvalues could be calculated decreases with increasing spin, the estimates are

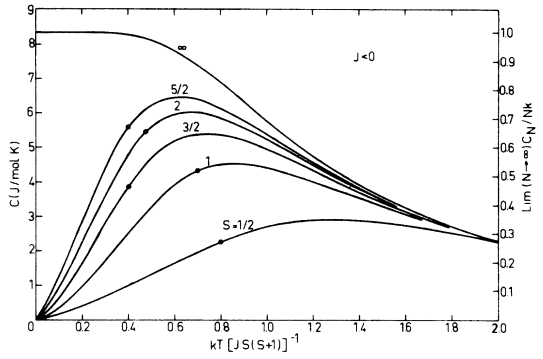

FIG. 7. Estimates of the specific heat of infinite chains with antiferromagnetic exchange for different spin as a function of reduced temperature. For each curve the temperature is indicated where the low-temperature polynomial is fitted in with the estimates obtained by direct extrapolation of the specific heat of finite chains.

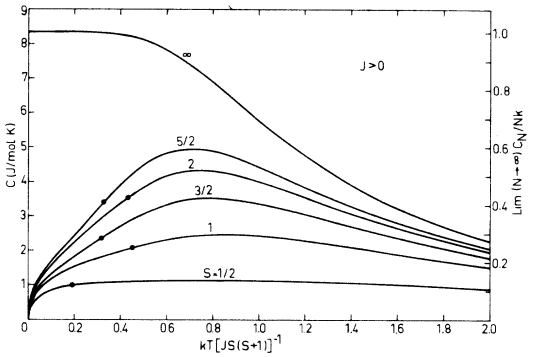

FIG. 9. Specific heat of infinite chains with ferromagnetic exchange for various spin. Above the dots the estimates are obtained by direct extrapolation of the specific heat of a number of finite chains (cf. Fig. 4). Below the dots the curves result from low-temperature polynomial fittings.

generally better for higher spin. This is not amazing since in the limit $S \to \infty$ the exact result is obtained from a combination of the data for two chains with length $N=2$ and $N=3$.

The entropy (Fig. 8) is plotted in reduced form $\eta^* = \eta/R \ln(2S+1)$ against reduced temperature T^*. Here too, there is a gradual increase with increasing S. The limiting curve for $S \to \infty$ is not known, because the limit of $\eta(S,T)/\ln(2S+1)$ for $S \to \infty$ cannot be calculated since the spin dependence of η is unknown in that limit.

C as well as η shows a smooth change with increasing S, also for low temperatures. Examination of Table IX, however, shows a difference in the low-temperature behavior between integer and half-integer spins. But the net result of the expression (31) is still regular.

The data for the ferromagnetic case are displayed in Figs. 9 and 10 for C and η^*, respectively. Here too the specific heat gradually approaches the limit-

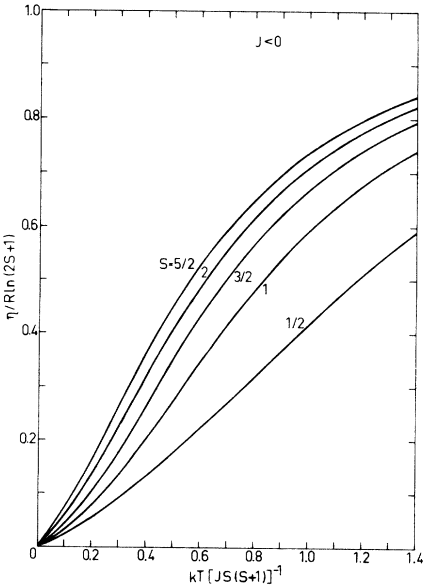

FIG. 8. Reduced entropy $\eta/R \ln(2S+1)$ as a function of reduced temperature for infinite antiferromagnetic chains with different spin.

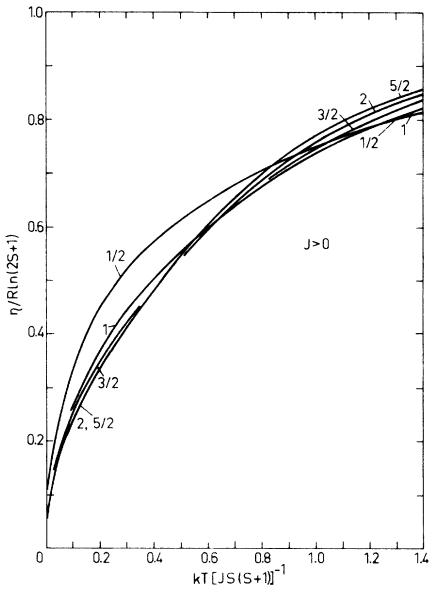

FIG. 10. Reduced entropy for chains with ferromagnetic exchange for various spin. The curves result from an integration of C/T when for C the estimates of Fig. 9 are used. For $T \to \infty$ all curves tend to unity.

ing curve for $S \to \infty$ with increasing S, and at the same time T_m^* decreases. In all cases (except $S = \infty$) the ferromagnetic specific heat is lower than the corresponding antiferromagnetic specific heat.

The specific heat for $J > 0$, unlike the case of $J < 0$, does show differences in overall shape between the integral and half-integral spins. For $S = \frac{3}{2}$ and $S = \frac{5}{2}$ (and possibly for $S = \frac{1}{2}$) a linear portion in C is observed below T_m, whereas for $S = 1$ and $S = 2$ the specific heat is curved in this region. We recall that this low-temperature part was fitted in with a polynomial in $T^{1/2}$, $T^{3/2}$, and $T^{5/2}$. Although such a form is not fully arbitrary—spin-wave theory also indicates these powers of T (Ref. 26)—it may be the cause of this linear portion. However, as mentioned, small changes are observed when varying the fitting temperature T_0. Even the use of other polynomials, such as one with $T^{1/2}$, T, and $T^{3/2}$, does not destroy this linearity. For integral S, on the other hand, the curved result is obtained in all cases, and with the alternative polynomials. Differences in the energy spectrum exist between half-integral and integral spins, even for the ground state (see Appendix), but we have no rigorous arguments to support the indicated differences in the specific heat.

The entropy (Fig. 10) also displays some differences but these are too small to be obvious in a plot. Striking is the over-all similarity of the entropy curves as compared to the antiferromagnetic data. With increasing spin the curves soon overlap and one might anticipate that the thermodynamic functions for ferromagnetic chains can more easily be scaled with respect to spin value than do the antiferromagnetic equivalents.

None of the figures with complete results (7–10) show error bars or otherwise indicate uncertainties in the estimates. Discussions in previous sections may help to establish some rules concerning the errors. For $T > 3T_m$ the high-temperature expansions rapidly converge in all cases and the results are undisputed. For $T_m < T < 3T_m$, the use of extrapolations from chains produces favorable results, and although errors are introduced in this way, the error estimate is of the order of 10^{-3}. The temperature T_0 is situated in a region where the extrapolations give rise to uncertainties of the order of 2% and between T_m and T_0 the errors gradually increase. Below T_0 error indication is very hard. The results for different T_0 show little variation [cf. Figs. 6(a) and 6(b)] but the resulting values for the parameters in (30) and (31) are quite sensitive to errors in C, $\partial C/\partial T$, and η at $T = T_0$. The situation is probably worst when $J < 0, S = \frac{1}{2}$. The difference from estimates of Bonner and Fisher is 20% near $kT/J = 0.1$ and 70% for $kT/J < 0.01$. The assumption that $b_1/R = 0.35$ (Bonner and Fisher) or $b_1/R = \frac{1}{3}$ (Takahashi[45]) for this situation would introduce an unrealistic peak in C for some temperature below $kT/J = 0.5$, unless we take C as large as possible within our error bounds for $kT/J > 0.8$. This indicates a possible error of 70% in b_1 for $S = \frac{1}{2}, J < 0$. For higher S the error is smaller and drops to the order of 5% for $S = \frac{5}{2}$. In the case of ferromagnetic coupling we can suggest an error of 5% in a_1 for all S. This would also be the error bound for the specific heat itself.

The specific heat of a ferromagnetic chain with $S = \frac{5}{2}$ offers a possibility of comparison with other techniques of evaluation. It was calculated by Rhodes and Scales[23] (RS) on the basis of a Green's-function approach. Weng,[21] using the results of Bonner and Fisher[15] for $S = \frac{1}{2}$ together with his own calculations for $S = 1$ and the exact result for $S \to \infty$,[7] used an interpolation to obtain estimates for other spins (the scheme is essentially a two-point Padé approximant, introduced by Baker et al.[29]).

Since for many properties $S = \frac{5}{2}$ is "quite close" to $S = \infty$, one may also use the formulas of Harrigan and Jones[47] that describe the assumed discrepancies from the $S = \infty$ curve. The estimated specific-heat curves that result from these three techniques are plotted in Fig. 11 together with our own result. In discussing the plot we first of all recall that our result is (nearly) errorless for $T > T_m$ since the Padé approximants to the high-temperature series as well as the direct extrapolation of finite chains rapidly converge. Weng's estimate (W) approaches this curve for sufficiently high temperatures, which is not surprising since his interpolation should be good if only a few terms in the HTE are of importance. For higher temperatures, the

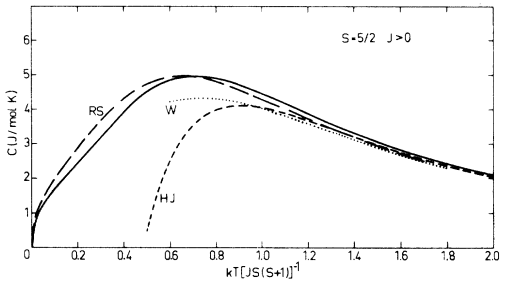

FIG. 11. Estimates from different techniques for the specific heat of an infinite ferromagnetic chain with $S = \frac{5}{2}$. The solid curve is the result of the present study (cf. Fig. 9). The line of dashes (RS) is the estimate of Rhodes and Scales obtained from Green's function analysis. Quantum corrections to the infinite-spin model by Harrigan and Jones are represented by the broken curve (HJ) and the dotted curve is an estimate obtained by Weng using an interpolation between the specific heat for $S = \frac{1}{2}$, $S = 1$, and $S = \infty$.

corrections for quantum effects (HJ) and the Green's-function result (RS) are both off by about 5% even at $T = 3T_m$. As emphasized by Harrigan and Jones, HJ is not valid at all for low temperatures, which is clearly visible. Also W deviates more and more at lower T. All in all, RS does show the same features as our estimate, including the linear part below T_m. However, the deviations between RS and our curve is 5% for $T > T_m$ and 15% for $T < T_m$. The same effect is observed for $S = \frac{1}{2}$ where the discrepancies between the GFA result and the estimates of Bonner and Fisher are large even at temperatures at which the latter are undisputed.[23]

Presentation of the results in their present form is hardly useful in experimental physics, where the curves are fitted to data points in order to check the one-dimensional character of the crystal under study and to determine the magnitude of J. For the high- and low-temperature parts the tables with coefficients in the respective series do suffice but the intermediate-temperature region is described poorly. To avoid comprehensive tables,[48] we shall use a formula from a preliminary paper to cover this temperature region.[37]

Guided by the expressions obtained from Padé-approximant representations of a series we adapted the estimated specific heat to a function F of the form

$$F(K) = \frac{a_2K^2 + a_3K^3 + a_4K^4}{(1 + b_1K + b_2K^2)^\gamma}, \tag{34}$$

with $K = \beta JS(S+1)$. The parameters are so chosen that

$$\int_{K_1}^{K_2} [F(K) - C(K)]^2 dK + \int_{K_3}^{K_4} [F(K) - C(K)]^2 dK \tag{35}$$

attains a mimimum value for given K_1, K_2, K_3 and K_4.

Since an expression of the form (34) should be valid in the complex K plane, we introduced two integrals in (35) in order to cover both sides of the real axis. By choosing K_1 and K_2 in the ferromagnetic domain and K_3 and K_4 in the antiferromagnetic region, we finished with a set of parameters for the function $F(K)$ such that $F(K)$ describes $C(K)$ favorably for both $J > 0$ and $J < 0$ for each S separately. The discrepancies between $F(K)$ and $C(K)$ are a function of the integration bounds. These boundaries are now chosen such that the maximum error between $F(K)$ and $C(K)$ in the integration intervals does not exceed 2%.

The values of the parameters and of the integration boundaries found in this way are summarized in Table XIII, for all S studied. The table also lists the values of T_m^*, the reduced temperature at which C reaches its maximum.

As was mentioned in the Introduction, actual magnetic crystals can hardly be expected to be of the pure Heisenberg type, nor will they be purely one-dimensional. This last restriction will affect the applicability of the presented results on the low-temperature side only, and for sufficiently small interchain interactions most of our estimates may still be used, as was shown in the recent analysis of the specific heat of $CsMnCl_3 \cdot 2H_2O$,[24,49] $\alpha RbMnCl_3 \cdot 2H_2O$ and $CsMnBr_3 \cdot 2H_2O$,[50] and TMMC.[51] Discrepancies from the Heisenberg form may change the overall specific heat quite drastically. For $S = 1$ we showed this for a Hamiltonian such as (1) with the additional single ion term Δ_z^2[22,49,52] and for $S = \frac{1}{2}$ Bonner and Fisher reviewed the anisotropic situation[15]. The results of these two papers together with the present analysis make it likely that equally good estimates may be obtained for any other Hamiltonian with $S \leq 5/2$. Recently Blöte[53] presented estimates for the specific heat of linear chains, obtained by a technique similar to the one described in Sec. IV B (direct extrapolation of finite chains). The Hamiltonian

TABLE XIII. Review of the values for the parameters in the formula $K = (a_2K^2 + a_3K^3 + a_4K^4)/(1 + b_1K + b_2K^2)^\gamma$ that fit best the calculated specific heat (C_∞), for different spin [cf. Eq. (35)]. The columns headed "interval" indicate the temperature region where the difference between F and C_∞ is less than 2%. The reduced temperature for which C_∞ reaches its maximum value is given in the columns headed T_m^*.

	Parameters						$J > 0$		$J < 0$	
S	a_2	a_3	a_4	b_1	b_2	γ	Interval	T_m^*	Interval	T_m^*
$\frac{1}{2}$	10.935	1.6555	2.8722	0.6900	1.7030	2.1765	1.06–4.0	0.88	0.95–4.0	1.32
1	10.745	−0.1034	1.0334	0.2450	0.8502	2.1078	0.59–2.8	0.85	0.56–4.0	0.86
$\frac{3}{2}$	10.939	−0.6760	0.6481	0.1047	0.6514	2.0792	0.50–4.0	0.80	0.50–4.0	0.75
2	11.072	−0.9653	0.4408	0.0408	0.6041	1.9449	0.40–4.0	0.75	0.50–4.0	0.67
$\frac{5}{2}$	11.097	−0.8511	0.1799	0.0195	0.5845	1.8081	0.38–4.0	0.71	0.36–4.0	0.62

studied by him contains also anisotropy in the exchange, and this does not influence the power of the technique. The detailed tables in Blöte's article were checked against our results. This reveals that the errors as estimated by Blöte are several orders of magnitude smaller than the errors that were assumed in the present study. A check for the case $S = 1$, using Padé approximants to the HTE of C as presented by Rushbrooke and Wood (Ref. 20), showed that the relative difference with Blöte's tables amounts to 2% in a region near T_m where his tables indicate an accuracy of 2×10^{-4}. Since in this region there is little reason to mistrust the Padé predictions, we conclude that Blöte has been too optimistic. Since his paper does not indicate the detailed way in which the estimates are obtained, it is hard to comment further on this point.

For $S > \frac{1}{2}$ the Hamiltonian may contain several parameters for the description of the zero-field splitting or the anisotropy in the exchange, and calculations on these general cases are therefore hard to present. When, as a result of different experimental techniques, a fair estimate exists for such parameters, calculations as those presented here are likely to give a proper theoretical estimate for comparison.

ACKNOWLEDGMENTS

The author wishes to acknowledge the considerable help and stimulating discussions with Professor P. van der Leeden, Professor C. Domb, and Dr. W. J. M. de Jonge. The constant cooperation of K. Kopinga and J. P. A. M. Hijmans is also gratefully appreciated.

APPENDIX: EXACTLY SOLVABLE RINGS AND CHAINS

The energy spectrum of a ring with $N = 3$ or $N = 4$ spins and of a chain with $N = 2$ or $N = 3$ can be solved exactly. These clusters are examples of the equivalent-neighbor Hamiltonian or the hypercubical Hamiltonian.

If $\mathcal{H}$ can be reduced to the form

$$\mathcal{H} = -J(\vec{R}^2 - n\vec{T}_1^2 - m\vec{T}_2^2), \tag{A1}$$

the eigenvalues may be labeled R, T_1, and T_2 since these are good quantum numbers.

For a chain with $N = 2$, we have $\vec{R} = \vec{S}_1 + \vec{S}_2$, $\vec{T}_1 = \vec{S}_1$, $\vec{T}_2 = \vec{S}_2$, $n = m = 1$, and accordingly the partition function is given by

$$Z_{\text{chain},2} = e^{-2KS(S+1)} \sum_{R=0}^{2S} (2R+1)e^{KR(R+1)} \tag{A2}$$

with $K = J/kT$. The ground-state energy per spin for the ferromagnet and the antiferromagnet may be calculated as

$$U(0)_{J<0} = S(S+1)J, \qquad U(0)_{J>0} = -S^2 J. \tag{A3}$$

A chain with three spins reduces to the form (A1), if we set $\vec{T}_1 = \vec{S}_2$, $\vec{T}_2 = \vec{S}_1 + \vec{S}_3$, $\vec{R} = \vec{T}_1 + \vec{T}_2$, and the partition function and ground-state energies are then

$$Z_{\text{chain},3} = e^{-KS(S+1)} \sum_{T=0}^{2S} e^{-KT(T+1)} \times \sum_{R=|T-S|}^{T+S} (2R+1)e^{KR(R+1)}, \tag{A4}$$

$$U(0)_{J<0} = \tfrac{2}{5}S(S+1)J \quad (-\tfrac{1}{4}J \text{ if } S \text{ half-integer}), \qquad U(0)_{J>0} = -\tfrac{4}{3}S^2 J. \tag{A5}$$

A ring with $N = 3$ may be written in the form (A1) if $\vec{T}_2 = \vec{S}$, $m = 3$, $n = 0$ and $\vec{R} = \vec{S}_1 + \vec{S}_2 + \vec{S}_3$ is substituted. The quantities are then

$$Z_{\text{ring},3} = e^{-3KS(S+1)} \sum_{T=S}^{3S} (2T+1)e^{KT(T+1)}, \tag{A6}$$

$$U(0)_{J<0} = S(S+1)J \quad (-\tfrac{1}{4}J \text{ if } S \text{ half-integer}), \qquad U(0)_{J>0} = -2S^2 J. \tag{A7}$$

For a ring with $N = 4$, $\vec{S}_1 + \vec{S}_3$ and $\vec{S}_2 + \vec{S}_4$ are good quantum numbers ($\vec{T}_1 = \vec{S}_1 + \vec{S}_3$, $\vec{T}_2 = \vec{S}_2 + \vec{S}_4$, $\vec{R} = \vec{T}_1 + \vec{T}_2$) and we find

$$Z_{\text{ring},4} = \sum_{T_1=0}^{2S} e^{-KT_1(T_1+1)} \sum_{T_2=0}^{2S} e^{-KT_2(T_2+1)} \times \sum_{R=|T_1-T_2|}^{T_1+T_2} (2R+1)e^{KR(R+1)}, \tag{A8}$$

$$U(0)_{J<0} = S(2S+1)J, \qquad U(0)_{J>0} = -2S^2 J. \tag{A9}$$

In order to calculate the trace of the graph $d_2(k)$ it is sufficient to calculate $\text{tr}(\mathcal{H}^k_{\text{chain},2})$, which is easily done from (A2). Since $\text{tr}(\mathcal{H}^k_{\text{chain},3}) = 2d_2(k) + d_3(k)$, $d_3(k)$ may be found from (A4) in combination with $d_2(k)$. No limitations are imposed on the order k.

The limiting high-temperature behavior of the specific heat per site may be found from (A2) and (A4) [using Eq. (18)],

$$C_{\text{chain},\infty} = 3C_{\text{chain},3} - 2C_{\text{chain},2}, \tag{A10}$$

a result that is correct to order β^5 for general spin. For $S \to \infty$ this expression is exact.

*Present address: Department of Aerospace Engineering, Delft University of Technology, Delft, The Netherlands.
[1]See, for instance, P. A. J. Tindemans and H. W. Capel, Physica (Utr.) 72, 433 (1974).
[2]See, for instance, L. J. de Jongh and A. R. Miedema, Adv. Phys. 23, 1 (1974).
[3]E. Ising, Z. Phy. 31, 253 (1925).
[4]For a review see C.J. Thomson, in *Phase Transitions and Critical Phenomena,* edited by C. Domb and M. S. Green (Academic, London, 1972), Vol. I.
[5]S. Katsura, Phys. Rev. 127, 1508 (1962).
[6]T. Nakamura, J. Phys. Soc. Jpn. 7, 264 (1952).
[7]M. E. Fisher, Am. J. Phys. 32, 343 (1964).
[8]H. E. Stanley, Phys. Rev. 179, 570 (1969); J. Appl. Phys. 41, 1278 (1970).
[9]See, for instance, H. E. Stanley, *Introduction to Phase Transitions and Critical Phenomena* (Oxford U. P., Oxford, England, 1971).
[10]T. Haseda and A. R. Miedema, Physica (Utr.) 27, 1102 (1961).
[11]R. B. Griffiths, Phys. Rev. 135, A659 (1964).
[12]For a review see G. S. Rushbrooke, G. A. Baker, and D. J. Wood, in Ref. 4, Vol III.
[13]D. D. Betts, C. J. Elliott, and M. H. Lee, Phys. Lett. 29A, 150 (1969); Can. J. Phys. 48, 1566 (1970).
[14]T. Obokata, I. Ono, and T. Oguchi, J. Phys. Soc. Jpn. 23, 516 (1967).
[15]J. C. Bonner and M. E. Fisher, Phys. Rev. 135, A640 (1964).
[16]R. Dingle, M. E. Lines, and S. L. Holt, Phys. Rev. 187, 643 (1969).
[17]R. E. Dietz, F. R. Merritt, R. Dingle, D. Hone, B. G. Silbernagel, and P. M. Richards, Phys. Rev. Lett. 26, 1186 (1971).
[18]T. Smith and S. A. Friedberg, Phys. Rev. 176, 660 (1968).
[19]H. Kobayashi, I. Tsujikawa, and S. A. Friedberg, J. Low Temp. Phys. 10, 621 (1973).
[20]G. S. Rushbrooke and P. J. Wood, Mol. Physics 1, 257 (1958).
[21]C. Y. Weng, Ph.D thesis (Carnegie Institute of Technology, 1968) (unpublished).
[22]T. de Neef and W. J. M. de Jonge, Phys. Rev. B (to be published).
[23]E. Rhodes and S. Scales, Phys. Rev. B 8, 1994 (1973).
[24]K. Kopinga, T. de Neef, and W. J. M. de Jonge, Phys. Rev. B 11, 2364 (1975).
[25]T. de Neef, Phys. Lett. 47A, 51 (1974).
[26]For example, see F. Keffer, in *Handbuch der Physik,* edited by S. Flügge (Springer, Berlin, 1966), Vol. 18, Pt. 2.
[27]See, for instance, A. Messiah, *Quantum Mechanics* (North-Holland, Amsterdam, 1970).
[28]C. Domb, Phil os. Mag. Suppl. 9, 34 (1960).
[29]G. A. Baker, Jr., G. S. Rushbrooke, and H. E. Gilbert, Phys. Rev. 135, A1272 (1964).
[30]G. S. Rushbrooke, J. Math. Phys. 5, 1106 (1964).
[31]W. Opechowski, Physica (Utr.) 4, 181 (1937).
[32]Our definition of graph differs here from the idea of diagrams as used by Rushbrooke and Wood (Ref. 20) and from the general use of graphs (Refs. 29, 30, 34, and 35). In following the definition of diagrams in Ref. 20, we may say that the sum of all diagrams that have the same topology—that is all diagrams that are the same if double bars are not distinguished from single bonds—is a graph as used in this paper. In the present work it is not useful to distinguish all diagrams, since in the calculation only a weighted sum is of importance. We did not like, however, to introduce a new term.
[33]N. Wirth, *Systematic Programming: An Introduction* (Prentice-Hall, Englewood Cliffs, N. J., 1973).
[34]G. S. Rushbrooke, G. A. Baker, Jr., and P. J. Wood, in Ref. 4, Vol. III.
[35]G. A. Baker, Jr., H. E. Gilbert, J. Eve, and G. S. Rushbrooke, Phys. Rev. 164, 800 (1967).
[36]For a review see D. S. Gaunt and A. J. Guttmann, in Ref. 4, Vol. III.
[37]L. P. Kadanoff, Physics (N.Y.) 2, 263 (1966).
[38]T. de Neef, A. J. M. Kuipers, and K. Kopinga, J. Phys. A 7, L171 (1974).
[39]D. D. Betts, C. J. Elliott, and M. H. Lee, Can. J. Phys. 48, 1566 (1970).
[40]K. Yamaji and J. Kondo, J. Phys. Soc. Jpn. 35, 25 (1973).
[41]J. Kondo and K. Yamaji, Prog. Theor. Phys. 47, 807 (1972).
[42]R. Kubo, Phys. Rev. 87, 568 (1952).
[43]M. Takahashi and M. Suzuki, Prog. Theor. Phys. 48, 2187 (1972).
[44]J. D. Johnson and B. McCoy, Phys. Rev. A 6, 1613 (1972).
[45]M. Takahashi, Prog. Theor. Phys. 50, 1519 (1973).
[46]W. Duffy, Jr. and K. P. Barr, Phys. Rev. 165, 647 (1968).
[47]M. E. Harrigan and G. L. Jones, Phys. Rev. B 7, 4897 (1973).
[48]A summary of the results presented here in tables and figures, is available as Eindhoven University of Technology Report No. THE/VVS/52075 (unpublished). This report also contains detailed tables of C_∞ in the intermediate-temperature region.
[49]T. de Neef, thesis (Eindhoven University of Technology, 1975) (unpublished).
[50]K. Kopinga (unpublished).
[51]W. J. M. de Jonge, C. H. W. Swüste, K. Kopinga and K. Takeda, Phys. Rev. B 12, 5858 (1975).
[52]J. V. Lebesque, T. de Neef and K. Kopinga (unpublished).
[53]H. W. J. Blöte, Physica (Utr.) 79B, 427 (1975).